Exploring spatiotemporal changes of the Yangtze River (Changjiang) nitrogen and phosphorus sources, retention and export to the East China Sea and Yellow Sea

Liu, X.; Beusen, A.H.W.; Beek, L.P.H.van; Mogollón, J.M.; Ran, X.; Bouwman, A.F.

Water Research 142 (2018) 246–255

Contents lists available at ScienceDirect

Water Research

journal homepage: www.elsevier.com/locate/watres

Exploring spatiotemporal changes of the Yangtze River (Changjiang) nitrogen and phosphorus sources, retention and export to the East China Sea and Yellow Sea

Xiaochen Liu [a, *], Arthur H.W. Beusen [a, b], Ludovicus P.H. Van Beek [c], José M. Mogollón [a, d], Xiangbin Ran [a, e], Alexander F. Bouwman [a, b]

[a] Department of Earth Sciences, Faculty of Geosciences, Utrecht University, P.O. Box 80021, 3508 TA Utrecht, The Netherlands
[b] PBL Netherlands Environmental Assessment Agency, P.O. Box 30314, 2500 GH The Hague, The Netherlands
[c] Department of Physical Geography, Faculty of Geosciences, Utrecht University, P.O. Box 80.115, 3508TC Utrecht, The Netherlands
[d] Institute of Environmental Sciences (CML), Leiden University, P.O. Box 9518, 2300 RA Leiden, The Netherlands
[e] Research Center for Marine Ecology, First Institute of Oceanography, State Oceanic Administration, 266061 Qingdao, PR China

ARTICLE INFO

Article history:
Received 31 March 2018
Received in revised form
27 May 2018
Accepted 3 June 2018
Available online 4 June 2018

Keywords:
Nutrient delivery
Mechanism model
Nutrient export
Nutrient retention
The Yangtze River
Source attribution

ABSTRACT

Nitrogen (N) and phosphorus (P) flows from land to sea in the Yangtze River basin were simulated for the period 1900–2010, by combining models for hydrology, nutrient input to surface water, and an in-stream retention. This study reveals that the basin-wide nutrient budget, delivery to surface water, and in-stream retention increased during this period. Since 2004, the Three Gorges Reservoir has contributed 5% and 7% of N and P basin-wide retention, respectively. With the dramatic rise in nutrient delivery, even this additional retention was insufficient to prevent an increase of riverine export from 337 Gg N yr^{-1} and 58 Gg P yr^{-1} (N:P molar ratio = 13) to 5896 Gg N yr^{-1} and 381 Gg P yr^{-1} (N:P molar ratio = 35) to the East China Sea and Yellow Sea (ECSYS). The midstream and upstream subbasins dominate the N and P exports to the ECSYS, respectively, due to various human activities along the river. Our spatially explicit nutrient source allocation can aid in the strategic targeting of nutrient reduction policies. We posit that these should focus on improving the agricultural fertilizer and manure use efficiency in the upstream and midstream and better urban wastewater management in the downstream subbasin.

1. Introduction

Nitrogen (N) and phosphorus (P) are essential nutrients required for living organisms and often limit primary production in terrestrial and aquatic ecosystems (Elser et al., 2007; LeBauer and Treseder, 2008). Modern human activities demand higher food and energy production, which helps accelerate N and P mobilization throughout the hydrosphere (Bouwman et al., 2009). Activities including fertilizer and manure use, fossil fuel consumption, the cultivation of leguminous crops, and wastewater discharge have more than doubled the rate at which biologically available nitrogen enters the terrestrial biosphere with respect to preindustrial levels (Galloway et al., 2008). This anthropogenic nutrient mobilization has led to eutrophication and oxygen-depletion of freshwater and coastal marine ecosystems (Diaz and Rosenberg, 2008), whose manifestations include changes in the structure of the food webs, loss of biodiversity, the eventual formation of toxic algae blooms, and a decline in fish production (Rousseau et al., 2000; Turner et al., 1998).

This change has been especially dramatic in China, where net N production increased from 9 Tg N yr^{-1} to 56 Tg N yr^{-1} from 1910 to 2010 (Cui et al., 2013; Gao and Wang, 2008; Howarth et al., 1996; Yan et al., 2010). In the Yangtze River basin (YRB), demographic growth and socioeconomic activities have risen drastically during the past century, especially since 1978. The total population dwelling by the main stream of the Yangtze River increased by 134% from 213 million in 1949 to 498 million in 2010 (Committee, 2014b). In the East China Sea, the frequency of harmful algal blooms (HABs) has increased by a factor of 3 every decade since the 1970s (Tang et al., 2006). In 2003, 119

* Corresponding author.
E-mail address: x.liu@uu.nl (X. Liu).

https://doi.org/10.1016/j.watres.2018.06.006

HABs events were reported in all Chinese coastal areas, of which 89% were in the East China Sea (China, 2009; Tang et al., 2006). Reported red tide occurrences in the Yangtze estuary region increased from 29 in the 1980s to 195 in the 2000s (China, 2009).

Existing studies of nutrient transport within the Yangtze River have primarily focused on the nutrient load at the river mouth (Dai et al., 2010; Li et al., 2007; Qu and Kroeze, 2012; Xu et al., 2013) or specific upstream monitoring stations or reaches (Cui et al., 2013; Duan et al., 2008; Tong et al., 2017; Wang et al., 2016; Yan et al., 2003; Zhiliang et al., 2003). Furthermore, these studies of YRB nutrient loading, retention, and export are either based on the measurements at Datong station or on subbasin-scale regression models that only stimulate one or two specific years.

Available studies lack spatiotemporal scales to analyze inter-annual patterns of river biogeochemistry and nutrient sources/exports under changing human pressures. In this paper we focus on the Yangtze River, the main water body draining into the East China Sea and Yellow Sea (ECSYS). This study uses the Integrated Model to Assess the Global Environment - Global Nutrient Model (IMAGE-GNM; Beusen et al., 2015), which couples models for hydrology and nutrient delivery to surface water with in-stream biogeochemistry and retention in a spatially explicit manner. We evaluate the changes in the various N and P sources and export to the coast for the period 1900–2010, with special attention to the impact of the Three Gorges Reservoir (TGR) (completed in 2004). Simulation results are compared to nutrient measurements from both upstream stations and the mouth. This study consists of two parts: (i) applying the model to identify the spatial distribution of nutrient sources and nutrient delivery for the upstream, midstream and downstream subbasins for the period 1900–2010, and (ii) analyzing the nutrient retention in water-bodies and export to ECSYS, including the effects of Three Gorges Dam (TGD).

2. Methods

2.1. Study area

The Yangtze River is the largest river in the Eurasian continent, covering an area of 1.8×10^6 km^2, with an average annual discharge of 892 km^3 for the period 1950–2010 (Committee, 2015) and a length of the main stream of 6400 km (Fig. 1). The YRB covers 20% of the Chinese land area, hosts 35% of the nation's population and receives 32% of the Chinese fertilizer inputs (Xing and Zhu, 2002). For our analysis, the YRB was divided based on watershed boundaries into three parts (Fig. 1), the upstream (upstream of Yichang), midstream (between Yichang and Hukou) and downstream (downstream of Hukou) subbasins (Wang et al., 2008).

2.2. IMAGE-GNM model

IMAGE-GNM is a spatially distributed model with an explicit 0.5-degree resolution. This grid cell-based model simulates the N and P delivery to surface water via surface runoff, shallow groundwater and deep groundwater. The IMAGE-GNM model couples the IMAGE integrated assessment model (Stehfest et al., 2014) with the global hydrological model PCR-GLOBWB (Van Beek et al., 2011). PCR-GLOBWB provides the water flux direction, discharge, surface water area, flooding area, lakes and reservoirs information, depth of water bodies and residence time of water bodies. IMAGE simulates the land use change and provides the climate data, and IMAGE-GNM calculates the soil N/P budget arising from diffuse sources (agricultural systems, natural systems, vegetation in flooded areas, deposition) and point sources (aquaculture, wastewater urban areas). After calculating retention in waterbodies (streams, rivers, floodplains, lakes, and reservoirs), each grid cell receives all the N and P output from all upstream cells

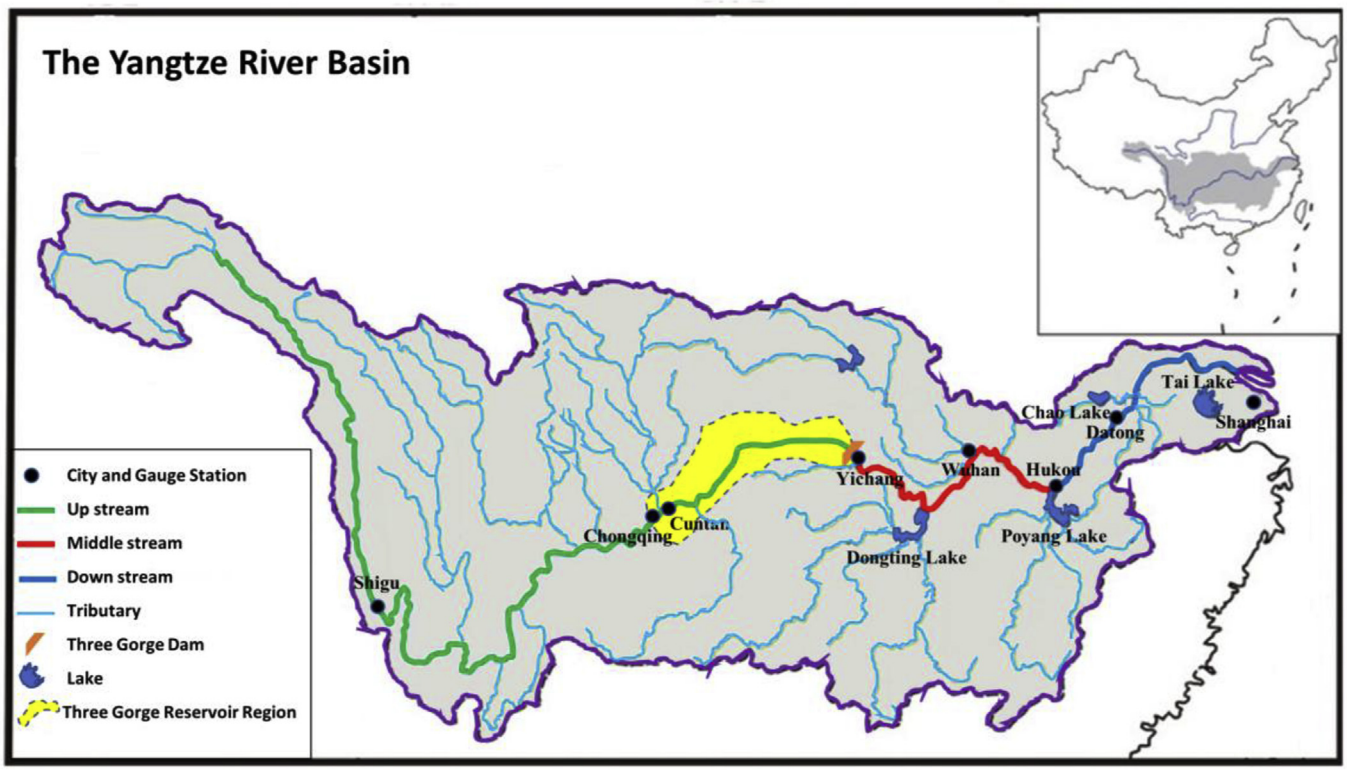

Fig. 1. Location of the monitoring stations in the Yangtze River basin.

and the N and P input from sources within the grid cell. For each grid cell, the nutrient and water flow pathway is given (Fig. SI1). Fig. SI2 indicates the data flows between PCR-GLOBWB and IMAGE. Additional details on the model are given in SI1.

IMAGE-GNM includes (i) N and P delivery from agricultural and natural land systems, via runoff to surface water and via leaching through shallow groundwater and deep groundwater, riparian zones and finally to surface water, (ii) N and P delivery from wastewater discharge and aquaculture, (iii) nutrient input from allochthonous organic material from vegetation in floodplains, (iv) N inputs from atmospheric deposition to terrestrial surfaces and water bodies, and (v) the nutrient spiralling method (Newbold et al., 1981; Wollheim et al., 2008) to calculate the in-stream N and P retention. For details on input and ancillary data we refer to Beusen et al., (2015). Land use and climate data are obtained from the IMAGE model (Stehfest et al., 2014).

Observations of annual discharge, concentrations of dissolved inorganic N (DIN, consisting of nitrate, ammonium and nitrite) and dissolved inorganic P (DIP) were collected from the Yangtze Water Resources Commission (CWRC) and published literatures (See SI2). Total N (TN) and total P (TP) concentrations were obtained by using TN:DIN and TP:DIP ratios from the literatures, see SI2. Nutrient input and output data were obtained from provincial-scale Chinese statistics (China 2014a, 2014b; Committee, 2014a). The start year depends on the data availability. When possible, we use 1961, otherwise the earliest available year. Missing years are interpolated. For years preceding the first available year, we combine the distribution of subnational data for the first available year together with FAO data for the whole country for the specific preceding year. If data for similar categories is available (e.g. livestock data for estimating feed use), the trend for that item is used to compute preceding years for the item with missing data. The provincial data are scaled so that the national total for China matches the FAOSTAT data (Bouwman et al., 2005). Data for the period 1900–1961 is from a recent study (Bouwman et al., 2013). We validated our model by calculating the root mean square error (RMSE) with respect to measured nutrient loads (see SI3.1).

The model sensitivity for the years 1900, 1950 and 2000 was investigated using the Latin Hypercube Sampling method, with uncertainty ranges for 48 input parameters for N and 34 for P (SI3.2). The standardized regression coefficient (SRC) was calculated to represent the relative sensitivity of output to the variations of model input parameters.

3. Results and discussion

3.1. Comparison with measurements

For the 1960–2010 period, the model predictions generally agree with the observed data at the monitoring stations (Fig. 2). The RMSE for the discharges are 20%, 24%, 10%, and 11% for the Cuntan, Yichang, Wuhan, and Datong stations, respectively. The modelled discharge matches better with the observations (Committee, 2014c) at downstream stations than at upstream stations. The annual trend is well represented, although the model slightly underestimates the discharge at Cuntan and Yichang stations.

The simulated TN load also agrees fairly well with observations (Fig. 2b,f,2h,2k). The RMSE for TN are 49%, 98%, 79% and 40% for the Cuntan, Yichang, Wuhan, and Datong stations, respectively. The uncertainty in the measurement data is shown by comparing different annual TN load estimates (Fig. 2n) obtained from different literature sources (SI2). The simulated TP load does not unreasonably deviate from the observed data at Datong (Fig. 2). The RMSE for TP are 226%, 238%, 227% and 62% for the Cuntan, Yichang, Wuhan and Datong stations, respectively. For the simulated period 1900–2010, there is a rapid increase of both the TN and TP loads after 1978 at all the stations, as is well reproduced by the model. However, we calculate on an annual basis, which may not appropriately capture short-term observations (due to, for example, flooding or dry months). Furthermore, the subbasins with a higher mismatch cover a smaller number of grid cells, which entails more uncertainty.

The discrepancy between simulations and observations for TP in upstream stations can be also partly attributed to the fixed TP/DIP ratio (Yang et al., 2008) used to estimate TP, which may be different for the various hydrogeological settings (e.g. sediment loads). However, these have not been measured for the different river segments or subbasins. Furthermore, the overestimation of the TP load may result from downscaling during the soil TP budget calculation and scarcity of measurements. This scaling problem arises as the provincial-wide fertilizer, livestock, and crop production data are allocated to grid cells with agricultural land use according to the IMAGE model. This may lead to overestimations for regions upstream of Cuntan where the actual dominant landscape is natural forest in mountainous areas (Su et al., 2017) (SI5, Movie SI3). The discrepancies between model and observations, however, do not affect our main conclusion that the agricultural fertilizer and manure use dominate in the upstream and midstream and point sources in the lower subbasin (see below).

3.2. Spatial-temporal variations of the nutrient sources

The whole-basin soil N budget increased almost 10 fold from 1.5 Tg N yr^{-1} in 1900 to 14.2 N Tg yr^{-1} in 2010 (Fig. 3a), particularly after 1970. With expanding agricultural activity and massive amounts of chemical fertilizer use, the soil N budget increased dramatically after 1980 in many parts of the YRB (SI5, Movie SI2). The soil P budget for the YRB went from slightly negative to 1.7 Tg P yr^{-1} for the period 1900–2010 (Fig. 3b). Prior to 1970, the P soil budget was negative in most grid cells, due to no fertilizer input and leading to soil P mining (SI5, Movie SI3). However, nutrient inputs may be underestimated as we did not include the use of human excreta in agriculture (FAO, 1977).

The nutrient soil budget, delivery, and river export (Fig. 3a and b) rapidly diverge after 1980, which results from N and P accumulation in soils and groundwater systems and the inability of the river biogeochemistry to retain the increasing nutrient delivery. Parallel to the nutrient budgets, the modeled N and P delivery to surface water in YRB was stable for the period 1900–1970, and started to accelerate after the 1970s in most places (SI5, Movie SI4, 5). Along with the increasing delivery since the 1970s, agricultural activities were the dominant source for N and P to the surface water in most parts of the YRB (SI5, Movie SI 6,7). Groundwater discharge from agricultural areas became the dominant N source in most grid cells and runoff from agricultural land became the dominant P source after 1970 (Fig. 3c). The sum of surface runoff and groundwater from land under natural vegetation was stable at about 325 Gg N yr^{-1} and 18 Gg P yr^{-1} during 1900–2010 (Fig. 3c). However, the share of these natural sources to total surface water delivery decreased sharply during this period from 52% to 5% for N and 16%–2% for P. In contrast, agricultural sources increased 31 fold from 221 Gg N yr^{-1} to 6791 Gg N yr^{-1} and 10 fold from 58 Gg P yr^{-1} to 587 Gg P yr^{-1} (Fig. 3d). The agricultural share of total delivery to rivers increased continuously from 38% to 83% for N and from 55% to 81% for P. These trends follow the Chinese agricultural development during the 20th century, which not only was the main economic driver during this period, but also saw a rapid technological increase after 1970s (Zhao et al., 2008).

The contribution of natural vegetation in floodplains decreased from 48 Gg N yr^{-1} to 28 Gg N yr^{-1} and from 4 Gg P yr^{-1} to 2 Gg P

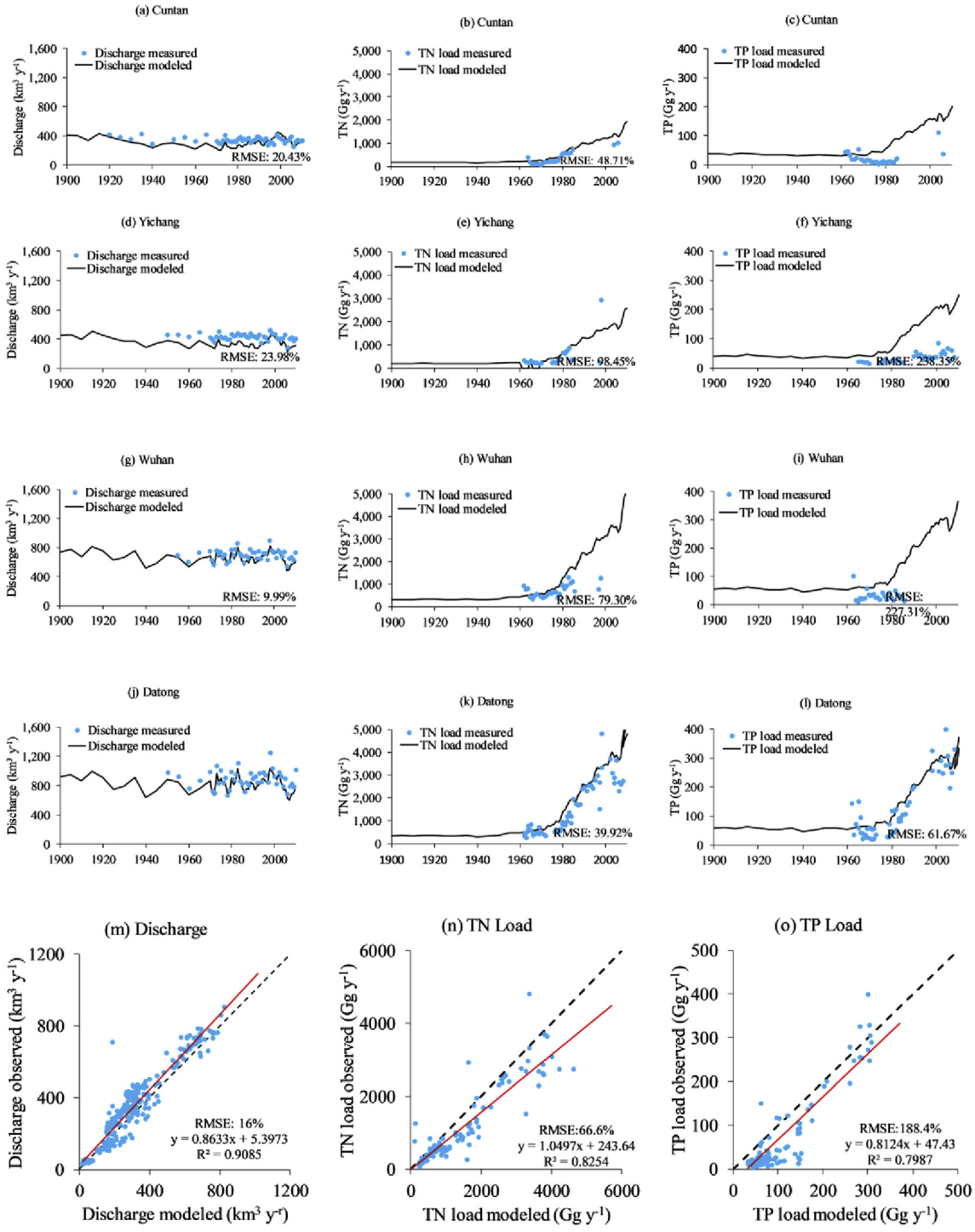

Fig. 2. Comparison of measurements (blue dots) and modeled (black line) discharge, TN load and TP load in the stations of Cuntan (a-c), Yichang (d-f), Wuhan (g-i) and Datong (j-l) for the period 1900–2010; and relationships between observed and modeled discharge, TN and TP loads for all data for all the stations (m-o). The black dashed line is the 1:1 line. (For interpretation of the references to colour in this figure legend, the reader is referred to the Web version of this article.)

yr^{-1} (Fig. 3c). Its share decreased from 8% to almost 0% for N and from 4% to almost 0% for P, mainly due to the increasing contribution from agricultural land and the construction of dams, which lead to a regulation of river discharge and thus decreasing flooding areas.

The contribution of point sources (sewage) for the 1900–2010 period increased three orders of magnitude from 2 Gg N yr^{-1} to 505 Gg N yr^{-1} and 0–64 Gg P yr^{-1}. With lagging wastewater treatment, rapid urbanization led to increasing amounts of untreated human waste which was discharged to surface water directly. The share of sewage increased from 1% to 9% for N and from 0% to 11% for P. The contribution of direct atmospheric deposition on waterbodies increased from 5 Gg N yr^{-1} to 57 Gg N yr^{-1}, but its share was stable due to the proportional increase of the total N sources.

Nutrients from aquaculture showed a dramatic increase from

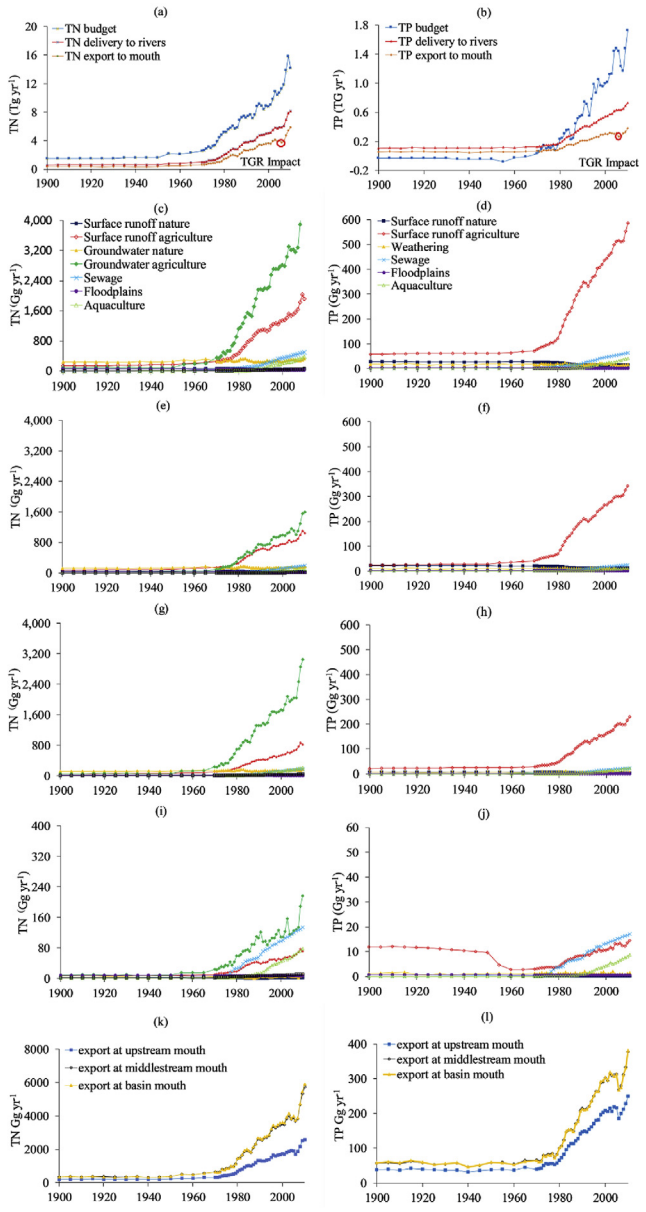

Fig. 3. (a) N and (b) P soil budget, loads to rivers and exports to mouth for the Yangtze river basin for the period 1900–2010; river TN and TP delivery to surface water from different sources for the period 1900–2010 for the whole basin (c,d), the upstream subbasin (e,f), the midstream subbasin (g,h), and the downstream subbasin (i,j); N and P export from the upstream, midstream and the whole Yangtze River basin during the period 1900–2010 (k,l).

1950 to 2010 of 1 Gg N yr^{-1} to 415 Gg N yr^{-1} and from 0 to 47 Gg P yr^{-1}. For this period, aquaculture's contribution to total delivery increased from 0% to 7% for N from 0% to 9% for P. This is also reflected in recent statistical trends for Chinese agriculture, with the contribution of fisheries steadily increasing its share within total agricultural production (Zhao et al., 2008).

The contribution of the various nutrient sources to the Yangtze River varied in different subbasins (Fig. 3; Fig. SI4,5,8). The shares of upstream and midstream to total N delivery for the whole YRB were about equal in 1900 (49% for upstream, 46% for midstream) with a small share of the downstream subbasin (5%), whereas the midstream subbasin became the main source of N delivery to surface waters from 1955. In 2010, 55% of the total N delivery to the Yangtze was from the midstream, and 39% from the upstream, and 6% from the downstream subbasin. The upstream subbasin was the main source of P delivery to the Yangtze with a stable share of around 57% during the period 1900–2010. The midstream and downstream subbasins saw a share change of P delivery from 35% to 39%, and from 11% to 6%, respectively.

Within the upstream subbasin, agricultural N sources (groundwater and surface runoff) became dominant from the 1970s, and N from sewage water became the third dominant source since around the year 2000 (Fig. 3e). P from surface runoff in agricultural areas remained the dominant source throughout the entire simulation period, and increased rapidly since 1980 due to the increasing use of fertilizer and manure from livestock (Bouwman et al., 2013) due to the increase of animal production. P from sewage (mid 1990s) started to exceed weathering and became the second dominant source, while other primarily natural sources remained stable, a direct consequence of increasing urbanization even in the upper portions of the YRB.

In the midstream subbasin, N from groundwater and surface runoff in agricultural areas started to increase rapidly in the 1970s. P delivery in the midstream subbasin follows the same trend as in the upstream subbasin, with sewage and aquaculture becoming the second and third dominant sources in the 1990s.

Results for the downstream subbasin are quite different from the upstream and midstream subbasins. N from groundwater in agricultural areas had been the dominant source in the downstream subbasin since the 1950s. N from sewage and groundwater in agricultural areas formed the dominant sources since the 1970s. P from surface runoff in agricultural areas was the dominant source, but its share in total P delivery decreased during the period 1900–1970 due to the shrinking agricultural areas. P from sewage and surface runoff in agriculture were the first and second dominant P sources since the 1980s. Aquaculture in the downstream subbasin has significantly increased nutrient delivery since 1990, becoming the third dominant source for P since 1992.

Groundwater receives nutrient inputs from leaching, especially in unconfined shallow aquifers under croplands (Puckett et al., 2011; Zhang et al., 2017). The residence times vary from years to decades or longer, and this means that large N and P amounts are temporarily stored in aquifers. This legacy implies that the surface water concentrations will persist for decades even after the fertilizer inputs have ceased (Sharpley et al., 2013; Van Meter et al., 2016). IMAGE-GNM accounts for the legacy of past agricultural N and P management. For N, legacies are related to the travel time of water and nitrate in aquifers, which typically exceeds the yearly timescale. In 1900, we calculated a temporary storage of 71 Gg N yr^{-1}, which rose to 3026 Gg N yr^{-1} in 2010, with a cumulative amount of 17797 Gg N over the whole 1900–2010 period. For P, IMAGE-GNM tracks all inputs and outputs in the soil P budget, which includes the effects of P accumulation and retention (from negative in 1900 to 1497 Gg P yr^{-1} in 2010) in soils. These nutrients may thus be released into the fluvial system in the coming decades, even if policies to reduce N and P overuse in agriculture are implemented now. GNM does not include direct manure discharge into the river, since we concluded that its influence on the N and P cycling in the YRB has been only minor in the 1970–2010 period and it is most probably declining due to government policies (see SI3.3).

3.3. Nutrient retention and export

3.3.1. Nutrient retention in waterbodies

The whole-basin retention in the Yangtze for 1900–2010 increased 9 fold from 239 Gg N yr^{-1} to 2252 Gg N yr^{-1} and 7 fold from 49 Gg P yr^{-1} to 348 Gg P yr^{-1} (Fig. 4a,c). In contrast, due to increasing N concentrations and the removal of electron donors,

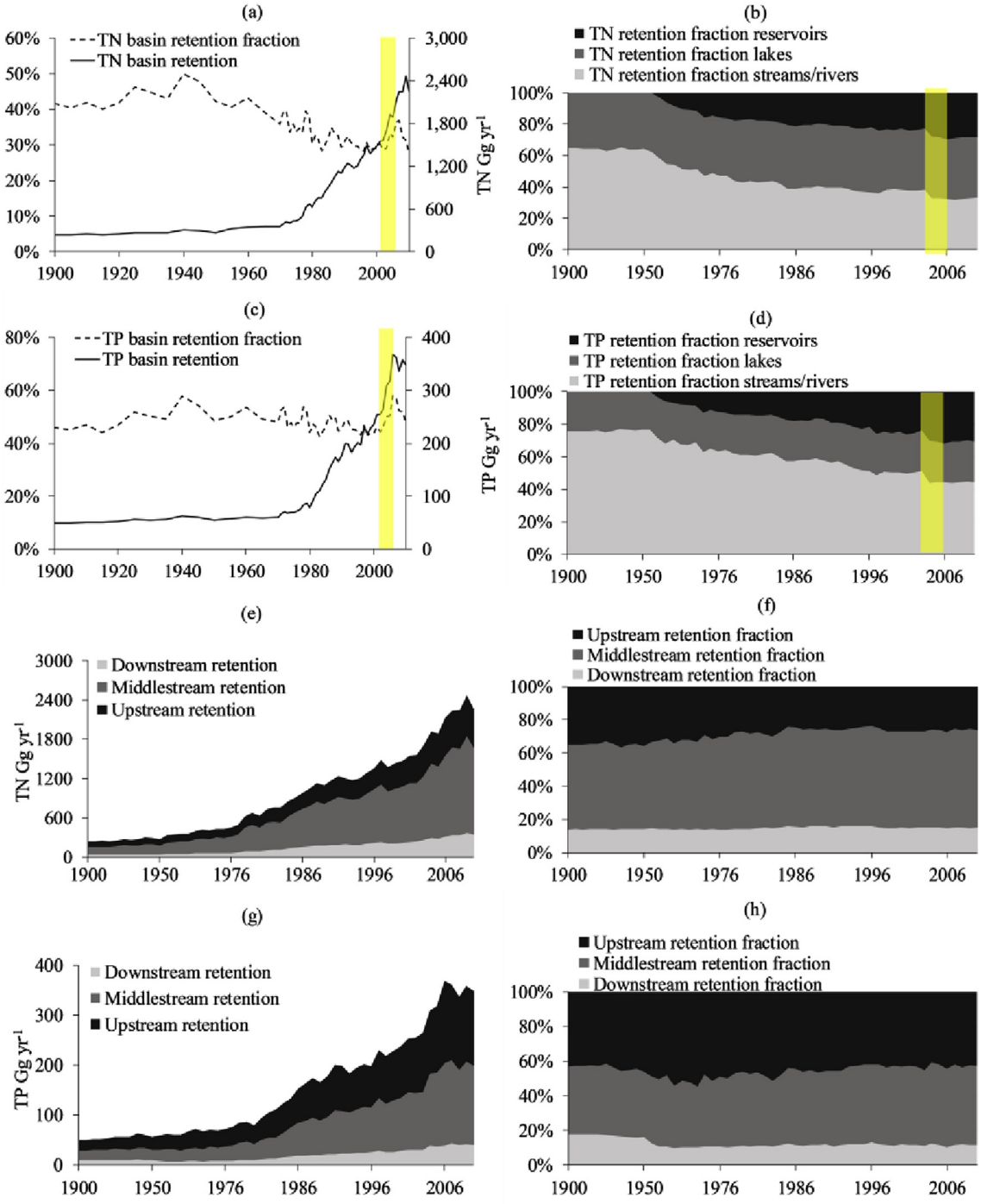

Fig. 4. (a) Total retention of N and the river basin N retention fraction, and (b) fraction of retention in streams/rivers, lakes and reservoirs in total basin; (c) total retention of P and the river basin P retention fraction, and (d) fraction of retention in streams/rivers, lakes and reservoirs in total basin. Yellow bar indicates the filling stage of the TGR; (e) Retention of N and (f) N retention fraction of midstream and downstream subbasins; (g) Retention of P and (h) P retention fraction of midstream and downstream subbasins for the period 1900–2010. (For interpretation of the references to colour in this figure legend, the reader is referred to the Web version of this article.)

denitrification rates dampened (equation 5) and thus the fraction of N retained decreased from 41% in 1900 to 28% in 2010. For P, it remained constant at 48% during the whole period (Fig. 4a,c).

During this same period, total retention in streams and rivers of the YRB increased from 155 Gg N yr^{-1} to 747 Gg N yr^{-1} and from 38 Gg P yr^{-1} to 154 Gg P yr^{-1}. However, the share of this retention decreased from 65% to 33% for N and from 76% to 44% for P (Fig. 4b,d). Total retention in lakes increased from 85 Gg N yr^{-1} to 863 Gg N yr^{-1} and from 12 Gg P yr^{-1} to 87 Gg P yr^{-1}, with the share of retention in lakes increasing from 35% in 1900 to 42% in 1996 and then decreasing to 38% in 2010 for N, while it remained steady at 24% during the entire 1900–2010 period for P (Fig. 4b,d). The retention in reservoirs increased rapidly from 0 to 642 Gg N yr^{-1} and from 0 to 107 Gg P yr^{-1}. The share of retention in reservoirs to the total retention increased from 0% to 28% for N and from 0% to 31% for P (Fig. 4b,d).

Total retention in the three subbasins increased both for N and P, but the fraction of nutrients removed in each subbasin has fluctuated (Fig. 4f,h). The upstream N retention fraction decreased from 35% in 1900 to 26% in 2010, increased from 51% to 58% in the midstream subbasin, and was constant at 15% in the downstream subbasin. For P, the contribution of upstream retention was constant at 46% throughout the period 1900 to 2010, increased from 39% to 46% for the midstream subbasin, and decreased from 18% to 11% for the downstream subbasin.

Total N retention in the TGR increased from 1 Gg N yr^{-1} in 2003 to 90 Gg N yr^{-1} in 2004 and from 0.2 Gg P yr^{-1} in 2003 to 20 Gg P yr^{-1} in 2004 (Fig. 5a and b). This increase in nutrient retention was mainly due to the infilling of the TGR, and contributed 5% for N and 10% for P of the nutrients load into the TGR (Fig. 3a and b). Our estimate of N retention is fairly close to the observation (6%) of TDN (the dominant form of N) in the TGR (Ran et al., 2017). The P retention is lower (circa 44%) than a measurement performed in April 2004 (Ran et al., 2016) but higher than a measurement (circa 4.91%) in 2003 when the TGR impoundment occurred (Sun et al., 2013). Due to the increase of N and P retention in the TGR, the N concentration increased by 39% from average 4.3 mg L^{-1} in 1900s to 6.0 mg L^{-1} after 2003 and the P concentration by 34% from 0.5 mg L^{-1} in 1900s to 0.7 mg L^{-1} after 2003 (Fig. 5c and d). The contribution of TGR to the whole-basin retention increased from 0% before impounding to approximately 5% for N and 6% for P after the impounding. The TGR reduced the nutrient load to the downstream part of YRB, but its differential nutrient retention may lead to a high risk of eutrophication within the reservoir itself.

3.3.2. Nutrient export to lower subbasin and the ECSYS

For the 1900–2010 period, the river N export at Yichang increased 13 fold from 196 Gg N yr^{-1} to 2562 Gg N yr^{-1} (17 fold 339–5714 Gg N yr^{-1} at Hukou, 17 fold 337–5896 Gg N yr^{-1} at the mouth) (Fig. 3k). The difference between Yichang and Hukou can be attributed to the increasing N contribution from the midstream subbasin. The N export to the ECSYS stems mainly from the midstream subbasin.

The P export at Yichang increased 7 fold from 37 Gg P yr^{-1} to 249 Gg P yr^{-1} (56–377 Gg P yr^{-1} at Hukou, 58–381 Gg P yr^{-1} at the river mouth) for the period 1900–2010 (Fig. 3l). The difference between Yichang and Hukou stations was smaller than for N export. This is largely due to the P export to the ECSYS, which stemmed mainly from the upstream subbasin.

The downstream subbasin contributes a small fraction of nutrient export to the ECSYS. This small share results from the small area of the downstream subbasin (only 5% of the whole YRB) while the water area of the downstream subbasin covers 19% of the whole water area. This leads to higher retention efficiency downstream, with our results indicating that 71% of local N (99% for P) delivery to surface water was removed in the downstream subbasin in the 2000s.

Nutrient export estimates from the Yangtze River to the ECSYS are available from various literature sources (SI6, Table SI5) for the year 2000. For N they vary from 1807 Gg N yr^{-1} (Lumped regression (Ti et al., 2012)) to 1132 Gg N yr^{-1} (Global NEWS-2 (Li et al., 2011; Mayorga et al., 2010; Seitzinger et al., 2005)) and 1142 Gg N yr^{-1} (MARINA model (Strokal et al., 2016a; Strokal et al., 2016b)). For P, they range from 95 Gg P yr^{-1} (Global NEWS-2 (Mayorga et al., 2010; Seitzinger et al., 2005)) to 172 Gg P yr^{-1} (MARINA model (Strokal et al., 2016a; Strokal et al., 2016b)). In contrast, our estimate of 3497 Gg N yr^{-1} and 296 Gg P yr^{-1} overshadow these values. If we use an observational reference of TN and TP concentration measurements combined with observed discharge in the Datong station, we obtain export values of 3698 Gg N yr^{-1} and 289 Gg P yr^{-1} (SI6) in 2002 (no observation available in 2000), which closely resemble our simulation estimates. There are several reasons for the discrepancy between the export calculations based on concentration and discharge to those of the statistical regression models. For one, the statistical analysis that served the basis for Global NEWS was based on discharge data from multiple rivers, and

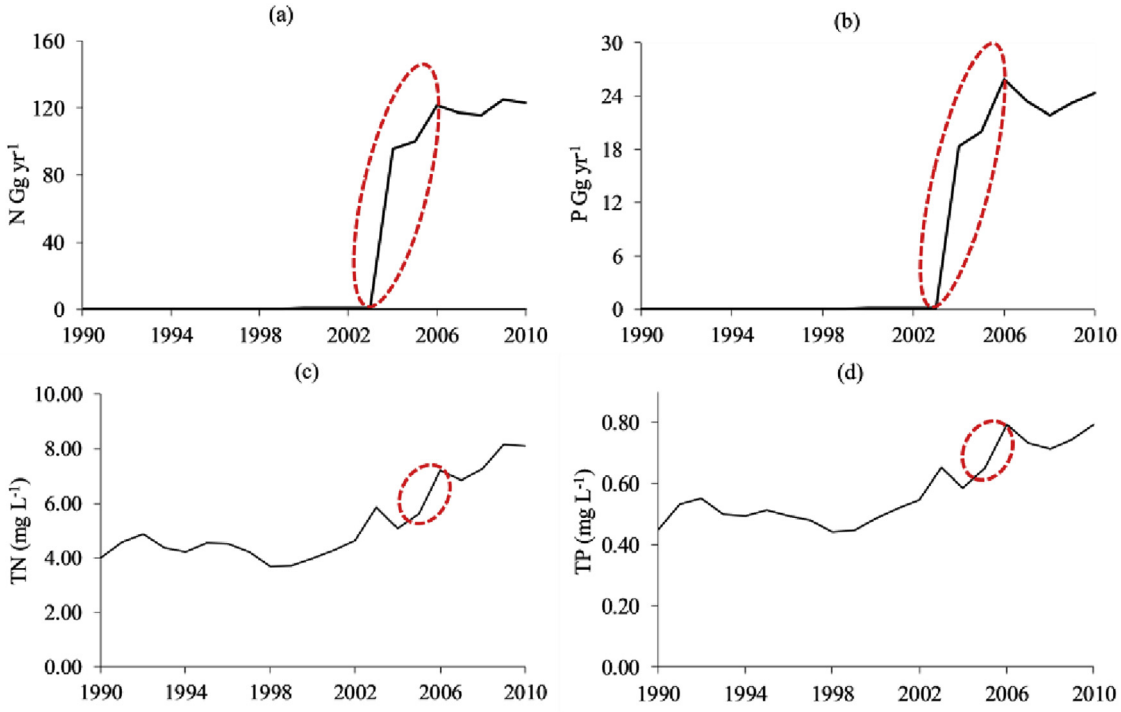

Fig. 5. N (a) and P (b) retention and TN (c) and TP (d) concentrations in the TGR for the period 1900–2010. The retention is calculated as the total for all grid cells covered by the TGR, and the concentration as the average of all TGR grid cells.

the Yangtze River may fall outside this global correlation. Furthermore, these lumped and statistical correlation models were calibrated with data from the Datong station (Li et al., 2011; Strokal et al. 2016a, 2016b; Ti et al., 2012; Yan et al., 2010), and ignore the contribution of the 600 km (Yang et al., 2002) river reach downstream of this station. The largest city group of China, the Yangtze River Delta Agglomeration, drains into this reach, and according to IMAGE-GNM, wastewater discharged into this reach is currently the dominant N and P source for the whole downstream subbasin. Our results show that the reach downstream of Datong contributes 78% of the total N export and 84% of total P export to the downstream subbasin, However, most of the N and P inflow is retained in the large areas of local water bodies such as Lake Tai. Consequently, this contribution represents a small fraction of the total N and P export to ECSYS (Fig. 3k and l).

Results from IMAGE-GNM closely match the monitoring data at Datong station despite not implementing direct animal manure discharge of N and P to surface waters, which we argue has been significantly overestimated in previous models of the YRB (see SI3.3). IMAGE-GNM can furthermore provide the direct nutrient export from Shanghai, the largest city of China, to the ECSYS. This value increased from 2.3 Gg N yr^{-1} to 99 Gg N yr^{-1} and from 0.3 Gg P yr^{-1} to 10 Gg P yr^{-1} for the period 1900–2010, mostly due to the rapid urbanization and development since the 1960s.

The sensitivity analysis shows that there is a shift of natural processes being the most important factors to agriculture becoming dominant in the course of the twentieth century (see SI3.2).

3.4. Implications for the ECSYS

Our results show that various human activities have become dominant drivers of the nutrient cycling in the YRB, especially since the 1970s. Agricultural practices dominate the nutrient delivery to the upper and middle subbasins, whereas point sources stemming from the Yangtze River Delta Agglomeration control those to the downstream subbasin (Fig. 3, Fig. SI7). Policies to reduce YRB nutrient concentrations should therefore focus on improving fertilizer and manure agricultural use efficiencies in the midstream and upstream subbasins and on improving urban wastewater management in the lower subbasin. The 17-fold increase in N export and 7-fold increase in P export imply a dramatic increase in the availability of nutrients and could lead to declining oxygen concentrations in coastal waters (Breitburg et al., 2018). Furthermore, due to increasing nutrient loadings and unbalanced nutrient retention in dams, the Yangtze River discharge to the ECSYS has seen a marked variation in its nutrient stoichiometry. Nutrient stoichiometry is an important indicator for the risk of HAB proliferation. The molar N:P ratio calculated for the mouth of the Yangtze in 1900 was 13, a value that is very close to the Redfield ratio (Redfield, 1934) (molar N:P = 16:1), indicating a healthy environment. However, in the year 2010 the water had a much higher N:P ratio of 35, indicating that exported water switched to P limitation. This change coupled to the decreasing silica (Si) export from the Yangtze River (Dai et al., 2011; Li and Chen, 2001) has caused a coastal imbalance in the loading of N, P and Si. When N and P are discharged in excess of Si with respect to the requirements of siliceous algae (diatoms), non-diatoms, often undesirable algal species, will develop (Billen and Garnier, 2007). HABs in both freshwaters and marginal seas in China are strongly related to these overall changing nutrient loads and ratios (Glibert et al., 2014). With a cumulative amount of 17797 Gg N stored in groundwater, and because policy efforts to reduce P loading to surface water are often more successful than strategies to reduce N flows (Bouwman et al., 2017), it will be very difficult to restore the nutrient stoichiometry to a “healthy” level (molar N:P = 16:1).

4. Conclusion

The model results from the dynamic, spatially explicit, mechanism non-calibrated IMAGE-GNM are in fair agreement with the measurements in the Cuntan, Yichang, Wuhan and Datong stations. To our knowledge, we have included the most comprehensive nutrients validation dataset covering from the upstream Cuntan station to the downstream Datong station for the period 1964–2010. This spatiotemporal simulations go beyond the finding from time-specific measurements and regression models calibrated to the Datong station nutrient data. This model thus elucidates the following findings:

- Our results reproduced the observed enormous increase of N and P export by the YRB to the ECSYS, particularly since the 1970s. The increase of nutrient retention in the YRB could not balance the increase of the nutrient delivery to the river.
- The contribution of TGR to the whole-basin retention increased from 0% before impounding to approximately 5% for N and 6% for P after the impounding. This additional retention after 2004 is insufficient to change the trend in the export due to the rapidly increasing N and P delivery to the streams. The TGR reduced the nutrient load to the downstream parts of the YRB, but this retention also implies an increasing risk of eutrophication within the reservoir itself.
- The modeled results indicate that the N export to the ECSYS stems mainly from the midstream subbasin, while P export is primarily from the upstream subbasin. The dominant source in the downstream subbasin is from sewage wastewater, most of the nutrients are sustained within the subbasin due to high fraction of water area. Dramatically increasing nutrients loads with high N:P ratio (molar N:P increase from 13 in 1900 to 35 in 2010) may be one of the reasons for the recent rapid increase in frequency and area coverage of harmful algal blooms in ECSYS.
- Policies to reduce the N and P export from the Yangtze river basin should focus on the midstream and upstream subbasins to improve fertilizer and manure use efficiencies. More concrete scenarios analysis should focus on the effectivity of current and future policies and regulations aimed at reducing nutrient sources in different parts of the YRB (i.e. where and how to reduce the anthropogenic nutrient inputs).

Acknowledgements

X.L. was funded by the China Scholarship Council and the National Natural Science Foundation of China grant 201306140029 and 41776089. J.M.M. was funded by Marie Skłodowska-Curie Individual Fellowship Grant no. 661163. A.F.B. and A.H.W.B. received support from PBL Netherlands Environmental Assessment Agency through in-kind contributions to The New Delta 2014 ALW projects no. 869.15.015 and 869.15.014.

Appendix A. Supplementary data

Additional information includes model output ascii files, figures, tables, model description, and movies (showing the spatially explicit changes of discharge, soil N and P budgets, N and P loads to streams, and dominant sources of N and P for the period 1990–2010).

Supplementary data related to this article can be found at https://doi.org/10.1016/j.watres.2018.06.006.

Reference

Beusen, A.H.W., Van Beek, L.P.H., Bouwman, A.F., Mogollón, J.M., Middelburg, J.J.,

2015. Coupling global models for hydrology and nutrient loading to simulate nitrogen and phosphorus retention in surface water – description of IMAGE–GNM and analysis of performance. Geoscientific Model Development 8 (12), 4045–4067.
Billen, G., Garnier, J., 2007. River basin nutrient delivery to the coastal sea: assessing its potential to sustain new production of non-siliceous algae. Mar. Chem. 106, 148–160 doi:110.1016.j.marchem.2006.1012.1017.
Bouwman, A., Beusen, A., Lassaletta, L., Van Apeldoorn, D., Van Grinsven, H., Zhang, J., 2017. Lessons from temporal and spatial patterns in global use of N and P fertilizer on cropland. Sci. Rep. 7, 40366.
Bouwman, A.F., Beusen, A.H.W., Billen, G., 2009. Human alteration of the global nitrogen and phosphorus soil balances for the period 1970–2050. Global Biogeochem. Cycles 23 (4), GB0A04.
Bouwman, A.F., Van Drecht, G., Van der Hoek, K.W., 2005. Global and regional surface nitrogen balances in intensive agricultural production systems for the period 1970-2030. Pedosphere 15 (2), 137–155.
Bouwman, L., Goldewijk, K.K., Van Der Hoek, K.W., Beusen, A.H., Van Vuuren, D.P., Willems, J., Rufino, M.C., Stehfest, E., 2013. Exploring global changes in nitrogen and phosphorus cycles in agriculture induced by livestock production over the 1900-2050 period. Proc. Natl. Acad. Sci. U. S. A. 110 (52), 20882–20887.
Breitburg, D., Levin, L.A., Oschlies, A., Grégoire, M., Chavez, F.P., Conley, D.J., Garçon, V., Gilbert, D., Gutiérrez, D., Isensee, K., 2018. Declining oxygen in the global ocean and coastal waters. Science 359 (6371) eaam7240.
China, M.o.A.o., 2014a. The Chinese Agricultural Statistical Report (In Chinese). Data Covering 1980-2011 Retrieved 8 October 2014. China Agriculture Press, Beijing, China.
China, N.B.o.S.o., 2014b. China statistical Yearbook (In Chinese). Data Covering 1981-2011 Retrieved 8 October 2014. China Statistic Press, Beijing, China.
China, S.O.A.o., 2009. Bulletin of Marine Environmental Quality of China data are available at: http://www.soa.gov.cn/chichao/index.html (Retrieved 10 December 2015).
Committee, C.L.Y.E., 2014a. China livestock Yearbook (In Chinese). Data Covering 1999-2011 Retrieved 8 October 2014. China Agriculture Press, Beijing, China.
Committee, C.P.S.Y.E., 2014b. China Population Statistics Yearbook (In Chinese). Data Covering 1949-2014 Retrieved 8 November 2014. China Statistics Press, Beijing, China.
Committee, C.S.B., 2015. Changjiang Sediment Bulletin. Data avaliable at. http://www.cjh.com.cn/ (Retrieved 8 October 2014).
Committee, C.W.R.C.E., 2014c. Yangtze River Yearbook (1992-2011). Changjiang Water Resources Commission.
Cui, S., Shi, Y., Groffman, P.M., Schlesinger, W.H., Zhu, Y.G., 2013. Centennial-scale analysis of the creation and fate of reactive nitrogen in China (1910-2010). Proc. Natl. Acad. Sci. U. S. A. 110 (6), 2052–2057.
Dai, Z., Du, J., Zhang, X., Su, N., Li, J., 2010. Variation of riverine material loads and environmental consequences on the Changjiang (Yangtze) Estuary in recent decades (1955– 2008). Environ. Sci. Technol. 45 (1), 223–227.
Dai, Z., Du, J., Zhang, X., Su, N., Li, J., 2011. Variation of riverine material loads and environmental consequences on the Changjiang (Yangtze) Estuary in recent decades (1955-2008). Environ. Sci. Technol. 45 (1), 223–227.
Diaz, R.J., Rosenberg, R., 2008. Spreading dead zones and consequences for marine ecosystems. Science 321 (5891), 926–929.
Duan, S., Liang, T., Zhang, S., Wang, L., Zhang, X., Chen, X., 2008. Seasonal changes in nitrogen and phosphorus transport in the lower Changjiang River before the construction of the Three Gorges Dam. Estuar. Coast Shelf Sci. 79 (2), 239–250.
Elser, J.J., Bracken, M.E., Cleland, E.E., Gruner, D.S., Harpole, W.S., Hillebrand, H., Ngai, J.T., Seabloom, E.W., Shurin, J.B., Smith, J.E., 2007. Global analysis of nitrogen and phosphorus limitation of primary producers in freshwater, marine and terrestrial ecosystems. Ecol. Lett. 10 (12), 1135–1142.
FAO, 1977. China: Recycling of Organic Wastes in Agriculture. Food and Agriculture Organization of the United Nations, Rome, p. 107.
Galloway, J.N., Townsend, A.R., Erisman, J.W., Bekunda, M., Cai, Z., Freney, J.R., Martinelli, L.A., Seitzinger, S., Sutton, M.A., 2008. Transformation of the nitrogen cycle: recent trends, questions, and potential solutions. Science 320, 889–892.
Gao, S., Wang, Y.P., 2008. Changes in material fluxes from the Changjiang River and their implications on the adjoining continental shelf ecosystem. Continent. Shelf Res. 28 (12), 1490–1500.
Glibert, P.M., Maranger, R., Sobota, D.J., Bouwman, L., 2014. The Haber Bosch–harmful algal bloom (HB–HAB) link. Environ. Res. Lett. 9 (10).
Howarth, R.W., Billen, G., Swaney, D., Townsend, A., Jaworski, N., Lajtha, K., Downing, J., Elmgren, R., Caraco, N., Jordan, T., 1996. Nitrogen Cycling in the North Atlantic Ocean and its Watersheds. Springer, pp. 75–139.
LeBauer, D.S., Treseder, K.K., 2008. Nitrogen limitation of net primary productivity in terrestrial ecosystems is globally distributed. Ecology 89 (2), 371–379.
Li, M., Xu, K., Watanabe, M., Chen, Z., 2007. Long-term variations in dissolved silicate, nitrogen, and phosphorus flux from the Yangtze River into the East China Sea and impacts on estuarine ecosystem. Estuar. Coast Shelf Sci. 71 (1–2), 3–12.
Li, M.T., Chen, H.Q., 2001. Changes of dissolved silicate flux from the Changjiang River into sea and its influence since late 50 years. China Environ. Sci. 21 (3), 1–5.
Li, X., Yang, L., Yan, W., 2011. Model analysis of dissolved inorganic phosphorus exports from the Yangtze river to the estuary. Nutrient Cycl. Agroecosyst. 90 (1), 157–170.
Mayorga, E., Seitzinger, S.P., Harrison, J.A., Dumont, E., Beusen, A.H., Bouwman, A., Fekete, B.M., Kroeze, C., Van Drecht, G., 2010. Global nutrient export from WaterSheds 2 (NEWS 2): model development and implementation. Environ. Model. Software 25 (7), 837–853.
Newbold, J.D., Elwood, J.W., O'Neill, R.V., Winkle, W.V., 1981. Measuring nutrient spiralling in streams. Can. J. Fish. Aquat. Sci. 38 (7), 860–863.
Puckett, L.J., Tesoriero, A.J., Dubrovsky, N.M., 2011. Nitrogen contamination of surficial aquifers-A growing legacy. Environ. Sci. Technol. 45 (3), 839–844.
Qu, H.J., Kroeze, C., 2012. Nutrient export by rivers to the coastal waters of China: management strategies and future trends. Reg. Environ. Change 12 (1), 153–167.
Ran, X.-b., Chen, H.-t., Wei, J.-f., Yao, Q.-z., Mi, T.-z., Yu, Z.-g., 2016. Phosphorus speciation, transformation and retention in the three Gorges reservoir, China. Mar. Freshw. Res. 67 (2), 173–186.
Ran, X., Bouwman, L., Yu, Z., Beusen, A., Chen, H., Yao, Q., 2017. Nitrogen transport, transformation, and retention in the Three Gorges Reservoir: a mass balance approach. Limnol. Oceanogr. 62 (5), 2323–2337.
Redfield, A., 1934. On the proportions of organic derivations in seawater and their relation to the composition of plankton (reprint). Benchmark Pap. Ecol. 1.
Rousseau, V., Becquevort, S., Parent, J.Y., Gasparini, S., Daro, M.H., Tackx, M., Lancelot, C., 2000. Trophic efficiency of the planktonic food web in a coastal ecosystem dominated by Phaeocystis colonies. J. Sea Res. 43 (3–4), 357–372.
Seitzinger, S., Harrison, J., Dumont, E., Beusen, A.H., Bouwman, A., 2005. Sources and delivery of carbon, nitrogen, and phosphorus to the coastal zone: an overview of Global Nutrient Export from Watersheds (NEWS) models and their application. Global Biogeochem. Cycles 19 (4).
Sharpley, A., Jarvie, H.P., Buda, A., May, L., Spears, B., Kleinman, P., 2013. Phosphorus legacy: overcoming the effects of past management practices to mitigate future water quality impairment. J. Environ. Qual. 42 (5), 1308–1326.
Stehfest, E., van Vuuren, D., Bouwman, L., Kram, T., 2014. Integrated Assessment of Global Environmental Change with IMAGE 3.0: Model Description and Policy Applications, Netherlands Environmental Assessment Agency (PBL). The Hague, available at: http://themasites.pbl.nl/models/image/index.php/Main_Page (Last access: 18 December 2015), 2014.
Strokal, M., Kroeze, C., Wang, M., Bai, Z., Ma, L., 2016a. The MARINA model (model to assess river inputs of nutrients to seAs): model description and results for China. Sci. Total Environ. 562, 869–888.
Strokal, M., Ma, L., Bai, Z., Luan, S., Kroeze, C., Oenema, O., Velthof, G., Zhang, F., 2016b. Alarming nutrient pollution of Chinese rivers as a result of agricultural transitions. Environ. Res. Lett. 11 (2).
Su, X., Yongyong, Z., Ming, D., Ruixiang, H., Yujian, Z., 2017. Spatial distribution of land use change in the Yangtze River Basin and the impact on runoff. Prog. Geogr. 36 (4), 426–436.
Sun, C., Shen, Z., Liu, R., Xiong, M., Ma, F., Zhang, O., Li, Y., Chen, L., 2013. Historical trend of nitrogen and phosphorus loads from the upper Yangtze River basin and their responses to the Three Gorges Dam. Environ. Sci. Pollut. Control Ser. 20 (12), 8871–8880.
Tang, D., Di, B., Wei, G., Ni, I.H., Im, S.O., Wang, S., 2006. Spatial, seasonal and species variations of harmful algal blooms in the South Yellow Sea and East China Sea. Hydrobiologia 568 (1), 245–253.
Ti, C., Pan, J., Xia, Y., Yan, X., 2012. A nitrogen budget of mainland China with spatial and temporal variation. Biogeochemistry 108 (1–3), 381–394.
Tong, Y., Bu, X., Chen, J., Zhou, F., Chen, L., Liu, M., Tan, X., Yu, T., Zhang, W., Mi, Z., Ma, L., Wang, X., Ni, J., 2017. Estimation of nutrient discharge from the Yangtze River to the East China Sea and the identification of nutrient sources. J. Hazard Mater. 321, 728–736.
Turner, R.E., Qureshi, N., Rabalais, N.N., Dortch, Q., Justic, D., Shaw, R.F., Cope, J., 1998. Fluctuating silicate:nitrate ratios and coastal plankton food webs. Proc. Natl. Acad. Sci. U. S. A. 95 (22), 13048–13051.
Van Beek, L.P.H., Wada, Y., Bierkens, M.F.P., 2011. Global monthly water stress: 1. Water balance and water availability. Water Resour. Res. 47 (7).
Van Meter, K.J., Basu, N.B., Veenstra, J.J., Burras, C.L., 2016. The nitrogen legacy: emerging evidence of nitrogen accumulation in anthropogenic landscapes. Environ. Res. Lett. 11 (3).
Wang, F., van Halem, D., van der Hoek, J.P., 2016. The fate of H2O2 during managed aquifer recharge: a residual from advanced oxidation processes for drinking water production. Chemosphere 148, 263–269.
Wang, H., Yang, Z., Wang, Y., Saito, Y., Liu, J.P., 2008. Reconstruction of sediment flux from the changjiang (Yangtze river) to the sea since the 1860s. J. Hydrol. 349 (3), 318–332.
Wollheim, W.M., Vörösmarty, C.J., Bouwman, A., Green, P., Harrison, J., Linder, E., Peterson, B.J., Seitzinger, S.P., Syvitski, J.P., 2008. Global N removal by freshwater aquatic systems using a spatially distributed, within-basin approach. Global Biogeochem. Cycles 22 (2).
Xing, G., Zhu, Z., 2002. Regional nitrogen budgets for China and its major watersheds. Biogeochemistry 57 (1), 405–427.
Xu, H., Chen, Z., Finlayson, B., Webber, M., Wu, X., Li, M., Chen, J., Wei, T., Barnett, J., Wang, M., 2013. Assessing dissolved inorganic nitrogen flux in the Yangtze River, China: sources and scenarios. Global Planet. Change 106 (0), 84–89.
Yan, W., Mayorga, E., Li, X., Seitzinger, S.P., Bouwman, A., 2010. Increasing anthropogenic nitrogen inputs and riverine DIN exports from the Changjiang River basin under changing human pressures. Global Biogeochem. Cycles 24 (4).
Yan, W., Zang, S., Sun, P., Seitzinger, S.P., 2003. How do nitrogen inputs to the Changjiang basin impact the Changjiang River nitrate: a temporal analysis for 1968-1997. Global Biogeochem. Cycles 17 (4), 2–1.
Yang, S.-l., Zhao, Q.-y., Belkin, I.M., 2002. Temporal variation in the sediment load of the Yangtze River and the influences of human activities. J. Hydrol. 263 (1), 56–71.

Yang, X., Xiong, B., Yang, M., 2008. Seasonal dynamics of phosphorus forms in water body and sediments of Nanhu Lake, Wuhan (in Chinese). Chin. J. Appl. Ecol. 19 (09), 2029–2034.
Zhang, J., Beusen, A.H.W., Van Apeldoorn, D.F., Mogollón, J.M., Yu, C., Bouwman, A.F., 2017. Spatiotemporal dynamics of soil phosphorus and crop uptake in global cropland during the 20th century. Biogeosciences 14 (8), 2055–2068.
Zhao, J., Luo, Q., Deng, H., Yan, Y., 2008. Opportunities and challenges of sustainable agricultural development in China. Philos. Trans. R. Soc. Lond. B Biol. Sci. 363 (1492), 893–904.
Zhiliang, S., Qun, L., Shumei, Z., Hui, M., Ping, Z., 2003. A nitrogen budget of the Changjiang river catchment. Ambio 32 (1), 65–69.